JMES The International Journal of
Mechanical Engineering and Sciences
https://iptek.its.ac.id/index.php/jmes
e-ISSN 2580-7471

Simple Bond-Graph Model To Predict Dried Material Temperature Evolution in A Batch Type Rotary Dryer

Sugeng Waluyo[1*], Ardiansyah[2], Nurul Latifasari[6],Condro Kartiko[4],Poppy Arsil[2], Rumpoko Wicaksono[3], Muhammad Syaiful Aliim[5] & Rifda Naufalin[3]
[1]Department of Industrial Engineering, Jenderal Soedirman University
[2]Department of Agricultural Engineering, Jenderal Soedirman University
[3]Department of Food Science and Technology, Jenderal Soedirman University
[4]Department of Software Engineering, Telkom Purwokerto Institute of Technology
[5]Department of Electrical Engineering, Jenderal Soedirman University
[6]Department of Food Science and Technology, Telkom Purwokerto Institute of Technology

Received: 23 November 2022, Revised: 30 September 2024, Accepted: 30 September 2024

Abstract

In this work, a model of temperature evolution inside a batch-type rotary dryer using the bond-graph method is proposed. The evolution model proposed here is mainly developed to predict dried material temperature inside the dryer during the drying process. The model is implemented in the 20-SIM bond-graph simulator (Controllab Products, the Netherlands) which shows realistic behaviors of the dried material temperature evolution with different combustion scenarios and rotation speeds. Here, using multi pulses heat generation, the dynamic changes of rotating dried material temperature can be modeled properly. The model proposed in this work can be used as an alternative tool to predict the behavior of a rotary dryer in a preliminary design stage.

Keywords: Rotary dryer, Batch type, Dried material, Temperature evolution, Bond-graph

1. Introduction

Drying is an important process in food production activities to maintain the stability of raw material compounds for a specific time period. For example, Effendi et al. [1] have found that higher drying temperature produces a higher enzyme inactivation process of the polyphenol oxidase enzyme during the processing of Kecombrang (Etlingera elatior) as raw material. Moreover, they also observed that if the drying temperature exceeded a particular temperature, polyphenol compounds in the dried material, i.e. Kecombrang, became unstable leading to the reduction of the compound.

Different types of drying methods have been widely used nowadays in food production processes. For example, Soodmand-Moghaddam et al. [2] use continuous force convection drying with the help of a belt conveyor running inside a heat chamber. Meanwhile, Naufalin et al. [3] have worked with a cabinet dryer to increase the production rate of the Kecombrang-based food products and maintain the quality of the products in the form of natural preservative powder. In contrast to drying methods, rotary dryers are mostly used due to their high efficiency. They can be found, for example in [4], which has developed an advanced rotary dryer based on infrared heating for fruit-based materials. Moreover, Tarhan et al. [5] use a rotary dryer for effectively drying peppermint plants controlled by constant and rectangular wave-shaped drying air temperature. Last but not least, Kaensup et al. [6] have tested a vacuum rotary dryer for chili under different chamber pressures and dryer rotational speeds.

Many existing bond-graph models for material drying considering temperature control can be found for example in [7–11]. They use the bond-graph model to represent complex interactions among physical parameters inside the drying equipment mainly by detailed modeling of heat transfer phenomena. For example, in Abbes and Mami [10], convective drying phenomena have been studied concerning drying efficiency due to heat losses to the environment and evaporation in dried materials. Concerning an overall production process, a rotary dryer can be modeled with a capacitive element as in [12, 13]. Unfortunately, none of them have considered the temperature evolution in dried materials as the main consideration and focus only on studying the thermal efficiency of a drying process.

As in some bio-based materials high temperature can destroy their compounds, as stated for example in [3], this work is aimed to develop a bond-graph model dedicated only to predicting temperature evolution in dried materials for a batch-type rotary dryer. The model is important

*Corresponding author. Email: sugeng.waluyo@unsoed.ac.id

as a tool to design an appropriate drying process that simultaneously reduces water content as well as preserves important compounds in the dried materials. Hence, the standard bond-graph model which uses temperature and heat transfer as effort and flow variables, respectively, is followed. Moreover, a novel approach is proposed here by defining additional resistance elements to represent heat transfer from the surface to the internal part of dried materials. Such an approach is necessary because temperature distributions in dried materials are not uniform in nature. Additionally, a novel mathematical fitting function is also proposed to consider the influence of the dryer rotation on temperature evolution in dried materials.

2. Thermal equilibrium in a batch-type rotary dryer

To obtain thermal equilibrium in a batch-type rotary dryer, it is necessary first to construct a proper model for heat transfers or flows generated by thermal sources and sinks, e.g. hot air and ambient temperature. To simplify three-dimensional (3-D) complex heat transfer problems in such dryer, only two-dimensional (2-D) cross-sectional heat transfer problem is considered as shown in Fig. 1 by assuming effective or average properties of the drying process along the dryer length. Meanwhile, the effect of dryer rotation on the thermal equilibrium will be captured by using the fitting function in a power-law form. One can find similar simplifications for instance in [14, 15].

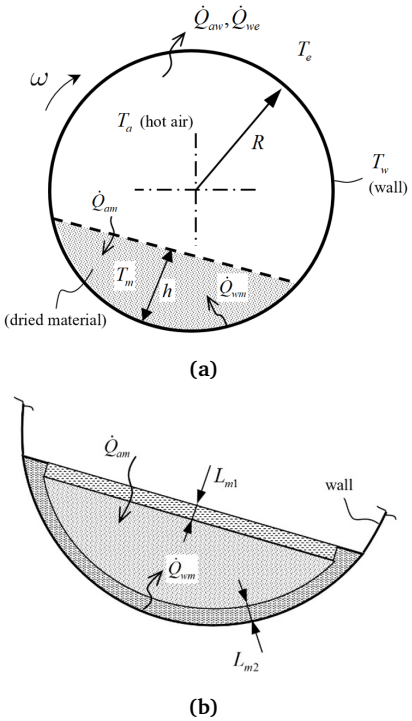

Figure 1. The proposed cross-sectional 2-D heat transfer model (a) for a batch-type rotary dryer with detailed heat flows in the dried material (b). The dried material height is defined by h.

It is obvious from Fig. 1 that there are 4 heat flows governing thermal equilibrium in the dryer due to the existence of dried material. The rate variables $\dot{Q}_{am}$ $\dot{Q}_{aw}$ $\dot{Q}_{we}$ $\dot{Q}_{wm}$are defined as heat flows from the hot air to the dried material, the hot air to the dryer wall, the dryer wall to the ambient temperature, and the dryer wall to the dried material, respectively. They are defined as

$$\dot{Q} = \frac{k_{m1}}{L_{m1}}(T_{ms} - T_m) + h_{am}A_m(T_a - T_{ms}) \quad (1)$$

$$\dot{Q_{aw}} = h_{aw}A_a(T_a - T_w) \quad (2)$$

$$\dot{Q_{we}} = h_{we}A_w(T_w - T_e) \quad (3)$$

$$\dot{Q_{wm}} = \frac{k_{m2}}{\phi L_{m1}}(T_w - T_m) \quad (4)$$

with A_a , A_w and A_m denoting the surface area of the inner wall free from the dried material, the outer wall, and the dried material exposed to the hot air, respectively. The other geometrical parameters are defined by L_{m1} L_{m2} $= \phi L_{m1}$ and as the thickness of effective layers of the dried material adjacent to the hot air and to the wall, respectively. It is assumed here that L_{m1} L_{m2} and can be approximated by each other to facilitate simple physical interpretations. Hence, the fraction ϕ is introduced such that $\phi\epsilon[0, 1]$. The layers are an important part of the bond-graph model because they provide us with a more accurate representation of the dried material temperature as a function of time. In both layers, the so-called effective thermal conductivities coefficient k_{m1} and k_{m2}, respectively, are defined.

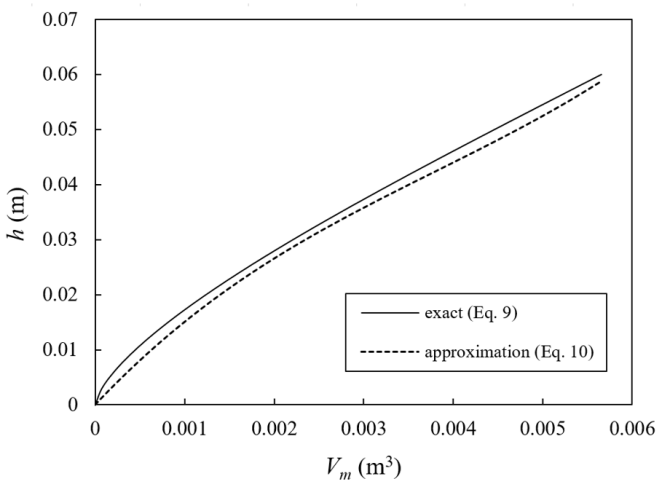

Figure 2. The exact and its corresponding approximation for the relation between V_m and h with $a = 2.12 \times 10^5 m^-8$, $b = -2.42 \times 10^3 m^{-5}$, and $c = 17.3m^{-2}$ for $l_m = 1.0m$ and $R = 0.06m$.

The other parameters related to the heat flow in Fig. 1 are defined as follows. Convection processes in the dryer are governed by $h_a m$ $h_a w$, and $h_w e$ represent the convection coefficients of the wall surface exposed to the hot air, on the surface of the dried material exposed to the hot air, and along the wall surface influenced by ambient temperature T_e, respectively. The variables T_m $T_m s$ T_a T_w are given as the temperatures, respectively, in the dried material, the surface of the dried material exposed to the hot air, the hot air, and inside the wall. Now, by assuming T_w is uniform and T_e is prescribed, one can determine T_m by solving simultaneously (1) - (4) with the help of the constant heat capacity of the hot air

$$Q_a = \rho_a V_a c_a (T_a - T_e) \tag{5}$$

In (5), a combustion process that produces heat Q_a to the hot air with its density, volume, and heat capacity defined by ρ_a, V_a and c_a, respectively, is modeled. On the other hand, it is assumed that the dried material and the wall have their heat own capacities, respectively, as

$$Q_m = \rho_m V_m c_m (T_m - T_{m0}) \tag{6}$$

$$Q_w = \rho_w V_w c_w (T_w - T_{w0}) \tag{7}$$

with T_{m0} and T_{w0} as the initial temperature of the dried material and the wall, respectively. The densities of the dried material and the wall are defined, respectively, by ρ_m and ρ_w, where to compute their corresponding masses, V_m and V_w are used to represent the volumes of the dried material and the wall, respectively.

According to Fig. 1, one has to evaluate h to obtain the dried material width exposed to the hot gas w_m by using

$$w_m = 2\sqrt{R^2 - (R-h)^2} \tag{8}$$

where R is the inner wall radius from the cross-section of the rotary dryer. Once w_m is obtained, the area of the dried material exposed to the hot air A_m can be computed easily. Now, the remaining problem is to find h from the dried material volume inside the dryer. Thus, it is necessary to solve the relation between h and the volume of hemispherical part of the rotary dryer V_m as shown in Fig. 1, namely

$$V_m = l_m \left[\cos^{-1}\left(\frac{R-h}{R}\right) R^2 \right] - (R-h)\sqrt{2Rh - h^2} \tag{9}$$

with l_m representing the length of the rotary dryer. Detail derivation of (9) can be found for instance in Weisstein [16]. Unfortunately, solving (9) directly for h as a function of in a close-form solution, as normally required in a bond-graph model, is not possible.

Hence, an alternative method may be proposed based on fitting with respect to a polynomial function by assuming that h can be approximated by

$$h = aV_m^3 + bV_m^2 + cV_m \tag{10}$$

The constants a, b, and c are determined by fitting the relation between V_m and h in (9) for the specific l_m and R. It is worth to note that the units of the constants in (10) follow their corresponding polynomial degree of V_m. For numerical tests later, the following constants are used, i.e. $l_m = 10m$ and $R = 0.06m$, to obtain the approximation for (9) based on (10) in Fig. 2, where the constants are given as $a = 2.12 \times 10^5 m^{-8}$, $b = -2.42 \times 10^3 m^{-5}$, and $c = 17.3m^{-2}$.

Now, with (8) and (10) in hand, the areas A_m and A_a can be computed as follows. While it simply introduces first

$$A_m = w_m l_m \tag{11}$$

to obtain A_m, an additional calculation to obtain A_a, i.e. the angle of material filling q, is given as

$$q = 2\cos^{-1}\left(\frac{R-h}{R}\right) \tag{12}$$

By using (12), one has

$$A_a = qRl_m \tag{13}$$

with q measured in radian. With the help of (13), the volume in (5) as $V_a = A_a l_m$ is obtained. The remaining geometrical variables are the wall volume given in (7) namely $V_w = \pi l_m \left[R^2 - (R - L_w)^2\right]$ and the outer area of the wall $A_w = 2\pi(R + L_w)l_m$ with L_w denoting the wall thickness.

Furthermore, it is worth to consider the dryer rotation speed ω as an additional parameter which affects not only heat flows but also temperature evolution in the dried material as studied in [16]. To account for ω in the proposed model, it is assumed that A_m can effectively change during rotation to A_{mix} according to the simple relation

$$A_{mix} = A_m \left(\frac{\omega}{\omega_0}\right)^{\beta} \tag{14}$$

There are two fitting constants in (14) which can be determined by using drying tests, i.e. ω_0 and β. In this work, the other geometrical and material properties depicted in Fig. 1 are considered independent concerning the dryer rotation to maintain the simplicity of the proposed model.

3. Bond-graph model

In this part, a bond-graph model is proposed based on the heat flows presented in Fig. 1. The model is dedicated only to predicting temperature evolution in the dried material with different thermal energy inputs Q_a.

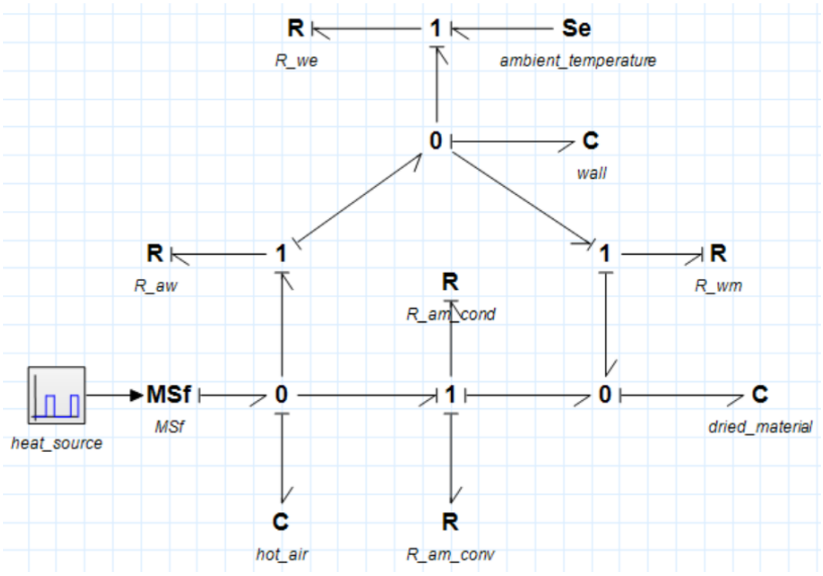

Figure 3. The proposed bond-graph model was implemented in the 20-Sim to simulate the temperature evolution of the dried material inside a batch-type rotary dryer.

Table 1. List of the bond-graph elements used in Fig. 3 according to their names

Symbol name	Type of element in bond-graph	Representation of
R*(R_am_cond)*	resistance (conduction)	Eq. 1
R*(R_am_conv)*	resistance (convection)	Eq. 1
R *(R_aw)*	resistance	Eq. 2
R *(R_we)*	resistance	Eq. 3
R *(R_wm)*	resistance	Eq. 4
C *(hot_air)*	capacitance	Eq. 5
C *(dried_material)*	capacitance	Eq. 6
C *(wall)*	capacitance	Eq. 7
Se *(ambient_ temperature)*	constant source	temperature outside dryer
heat_source	signal source	combustion as a function of time

The model proposed here is given in Fig. 3 and implemented in the 20-SIM software from the Controllab Products Netherlands developed by [17]. The **MSf** (modulated source flow) element works by translating the unit input signal to model the heat source element Q_a. While in zero junction **0** temperature is distributed equally to all branches, in one junction **1** heat flows in equal amounts to all branches. The other bond-graph elements in Fig. 3 are described in Table **??**. In order to fit with the purpose of this study, the elements are modified from their standard version in the software which does not contain the formulations depicted in (1) to (7).

In Fig. 3, the dried material is considered a capacitance element where it is capable of storing heat from the hot air and the wall simultaneously. It is applied also to the wall and the hot air. In the bond-graph model, the capacitances contribute to effort variables where temperatures are assumed constant in the whole part of their corresponding physical components, i.e. the hot air, the wall, and the dried material. In the model, it assumed that the heat transfers to the wall, the hot air, and the environment are dominated only by convection processes as indicated by (2) and (3).

In the context of heating the dried material, the proposed model can be described as follows. A heat source from a combustion nozzle heats the air inside the dryer at a specific time. Heat from the hot air flows along different paths to the dried material either through the wall or directly from the dried material surface exposed to the hot air. Meanwhile, heat from the hot air also flows to the environment, i.e. the ambient temperature, through the outer surface of the dryer wall. From the overall process described here, the bond-graph model will predict temperature evolution in the dried material concerning the time-dependent heat source types.

Table 2. Material and geometrical constants for the numerical tests

Constants (units)	Value	Constants (units)	Value
$k_{m1}(W.m^{-1}.K^{-1})$	0.2	$T_{w0}(K)$	303
$L_{m1}(m)$	0.05	$T_{m0}(K)$	303
$h_{am}(W.m^{-2}.K^{-1})$	0.2	$c_m(J.kg^{-1}.K^{-1})$	1
$h_{aw}(W.m^{-2}.K^{-1})$	5	$\rho_w(kg.m^{-3})$	7000
$T_e(K)$	303	$c_w(J.kg^{-1}.K^{-1})$	10
$h_{we}(W.m^{-2}.K^{-1})$	0.04	$\omega_0(rad)$	1.25
$k_{m2}(W.m^{-1}.K^{-1})$	0.069	$\beta(-)$	-0.5
$\phi(-)$	0.4	$l_m(m)$	1
$\rho_a(kg.m^{-3})$	1.25	$V_m(m^3)$	0.05
$c_a(J.kg^{-1}.K^{-1})$	100	$\rho_m(kg.m^{-3})$	200
$L_w(m)$	0.05	$T_{a0}(K)$	303

4. Numerical Tests

In this part, numerical tests are conducted to study the behavior of the bond-graph model under pulse signals which represents short and multiple combustions from a heat source inside the dryer. The use of short combustion is normally found in many dryers as an effort to maintain drying temperature at a specific level set by using control

mechanisms. On the other hand, multiple combustions are used to model heat accumulation in the capacitance elements which must be correctly represented by the proposed model. Relied on both heat source types, a primary study can be focused on the temperature evolution in the dried material and its effect on the hot air temperature. Material and geometrical constants used in the tests are given in Table **??**.

First, a short pulse signal is used to represent a single combustion burst into the air inside the rotary dryer. The proposed model gives the responses shown in Fig. 4 for the temperature in the dried material and the hot air as functions of time. One can observe that the temperature in the dried material increases as the hot air temperature decreases up to equilibrium states represented by their corresponding initial temperatures. Furthermore, the influence of rotation on the drying performance can be also seen in Fig. 4 where the reduction of the rotation speed gives the lower value of the maximum temperature in the dried material as also studied by [14]. In the case of opposite behaviors due to ω observed in real experimental works, one may use different values of ω_0 and β apart from their values in Table **??**. From the tests here it is verified that the proposed bond-graph model can represent the fundamental principle of heat transfer, i.e. heat flowing from high temperature to the lower one up to equilibrium states.

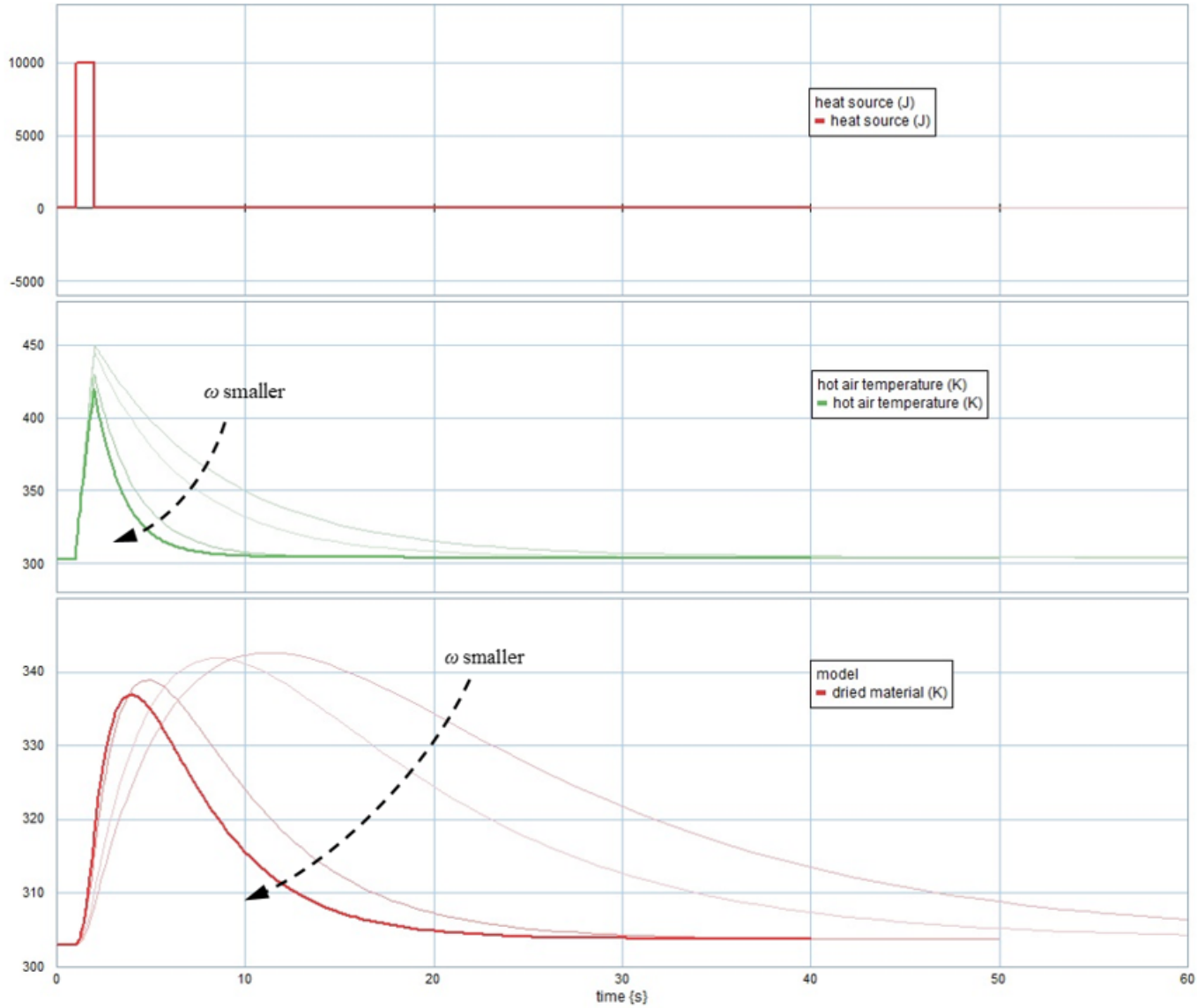

Figure 4. Plots of the simulation results from the proposed model are depicted in Fig. 3 by using single pulse combustion scenarios. The effect of the dryer rotation ω is also presented here. While the unit for the heat source is Joule (J), the temperatures in the hot air and the dried material are defined in Kelvin (K).

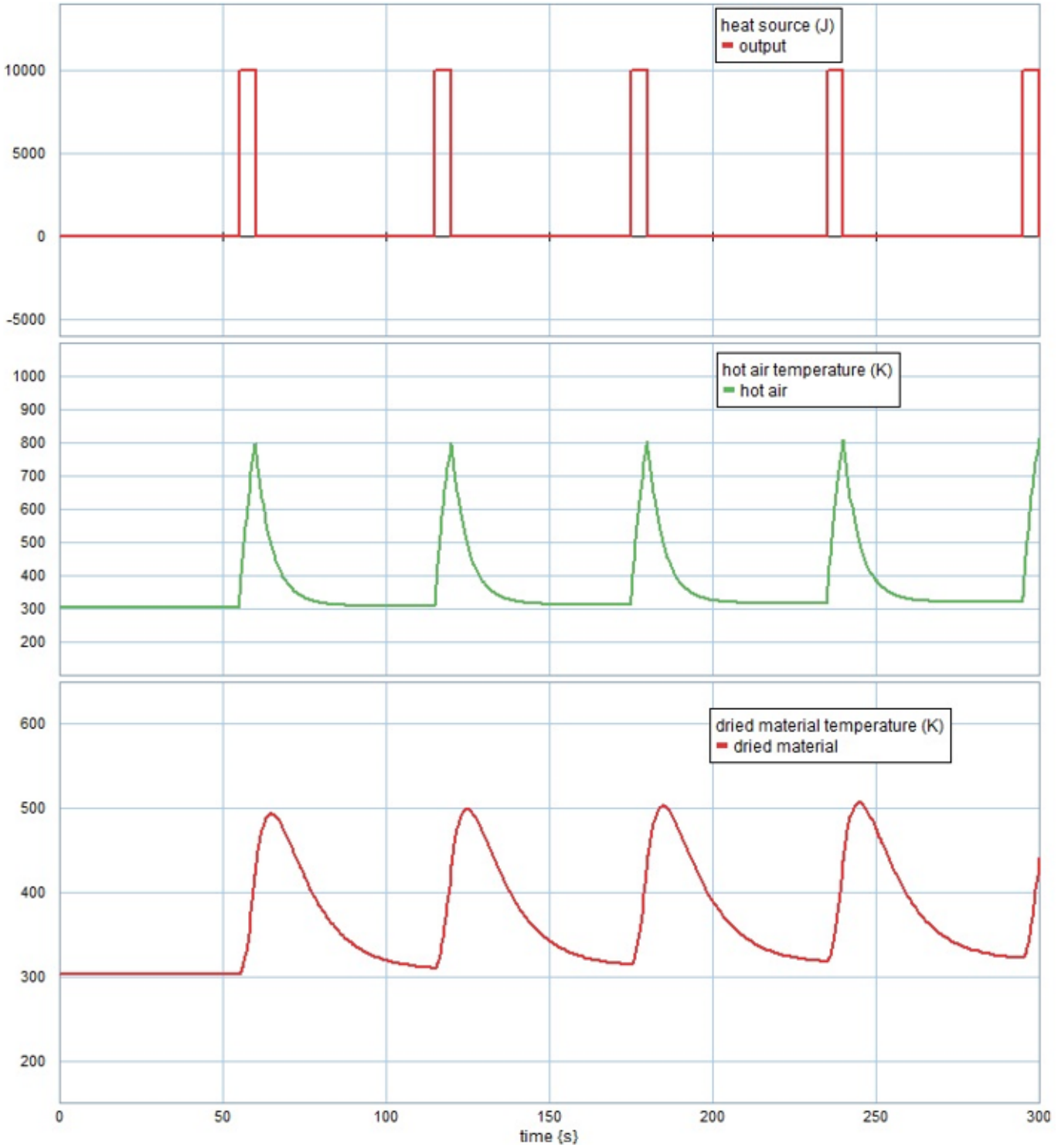

Figure 5. Plots of the simulation results from the model depicted in Fig. 3 by using a low-frequency multi-pulses combustion scenario.

In the second case, a series of combustion bursts with different intervals are used to show the capability of the model to predict heat accumulation in the dried material. When it occurs, there are possibilities of overheating and, simultaneously, reducing the quality of the dried material. Figs. 5 and 6 show that temperature in the dried material increases if the combustion interval is close enough and vice versa. It means that heat flows to the environment through the wall is slower than heat accumulated in the hot air due to the combustions. This verifies that the proposed model can also be used to predict the possibility of overheating in the dried material. Thus, the proposed model is appropriate as a tool for drying simulation before the actual drying process is performed.

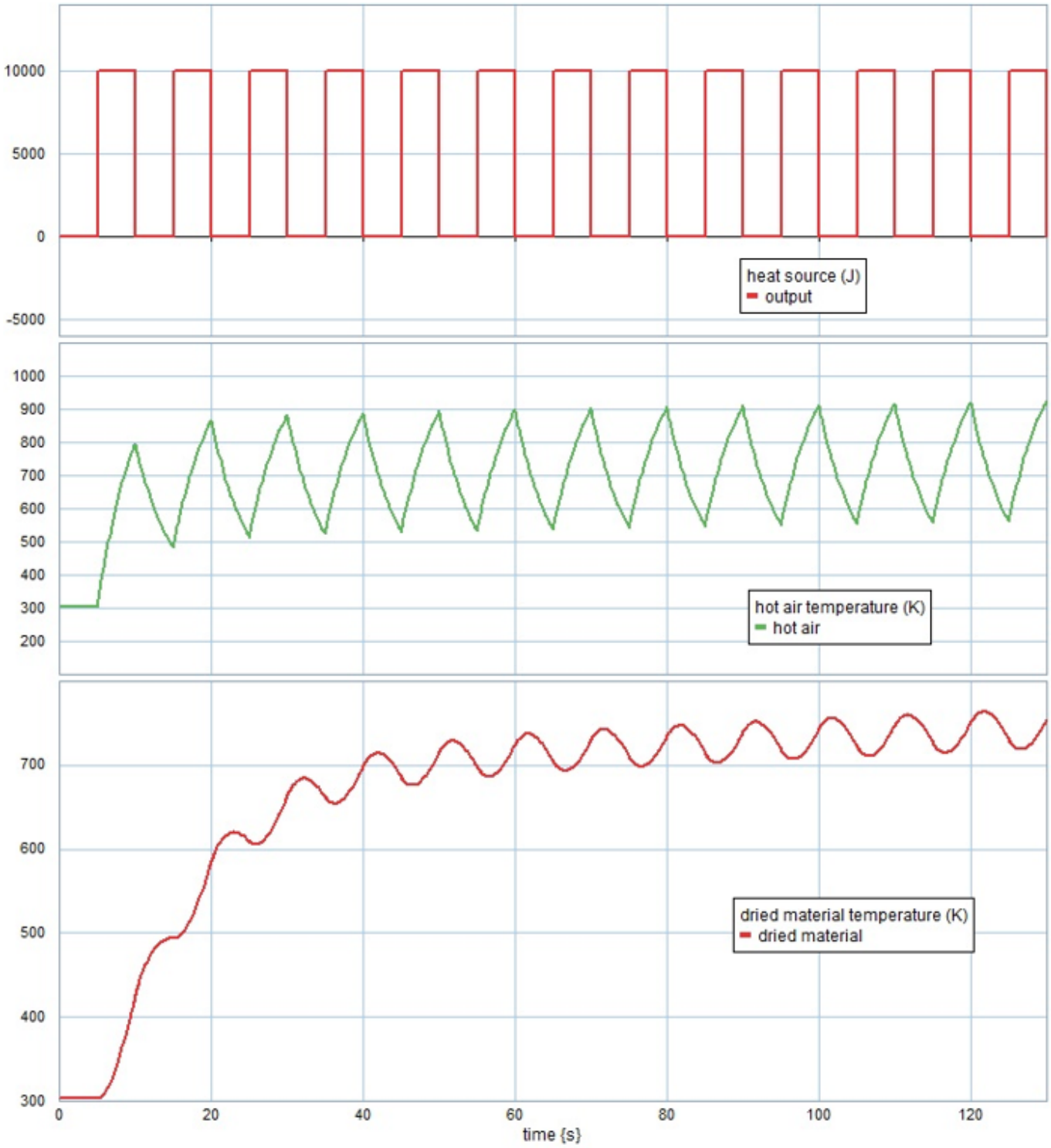

Figure 6. Plots of the simulation results from the model depicted in Fig. 3 by using a high-frequency multi pulses combustion scenario.

In the second case, a series of combustion bursts with different intervals are used to show the capability of the model to predict heat accumulation in the dried material. When it occurs, there are possibilities of overheating and, simultaneously, reducing the quality of the dried material. Figs. 5 and 6 show that temperature in the dried material increases if the combustion interval is close enough and vice versa. It means that heat flows to the environment through the wall is slower than heat accumulated in the hot air due to the combustions. This verifies that the proposed model can also be used to predict the possibility of overheating in the dried material. Thus, the proposed

model is appropriate as a tool for drying simulation before the actual drying process is performed.

Provided with the results from Figs. 5-6, the model is ready to be used for further verification works concerning actual drying experiments by using a batch-type rotary dryer. Unfortunately, such verifications are split from this current work because the determination of variables ω_0, β, ϕ, L_{m1}, k_{m1}, k_{m2},and h_{am} simultaneously from the experiments are time-consuming and require separate works.

5. Conclusions

A bond-graph model to predict temperature evolution in the dried material inside a batch-type rotary dryer is developed here. In the numerical test, it is shown that the model can represent heat flows from and to the dried materials either by using single-pulse or multi-pulse combustion scenarios. Moreover, the model is also capable of representing the effect of the dryer rotation on the temperature evolution simply by using the fitting function. With such a model, a batch-type rotating dryer can be designed properly to find its best configuration to maintain the quality of the drying products in particular during a preliminary design stage.

6. Acknowledgments

We would like to thank you for the financial support from Lembaga Pengelola Dana Pendidikan (LPDP) Republik Indonesia through the RISPRO Invitation Program 2020-2022.

References

[1] K. Effendi, N. Fauziah, R. Wicaksono, E. Wuryatmo, P. Arsil, and R. Naufalin, "Analysis of bioactive components and phytochemical of powders stem and leaves of kecombrang (etlingera elatior)," *IOP Conference Series: Earth and Environmental Science*, vol. 406, p. 012003, 12 2019.

[2] S. Soodmand-Moghaddam, M. Sharifi, H. Zareiforoush, H. Mobli, *et al.*, "Mathematical modelling of lemon verbena leaves drying in a continuous flow dryer equipped with a solar pre-heating system," *Quality Assurance and Safety of Crops & Foods*, vol. 12, no. 1, pp. 57–66, 2020.

[3] R. Naufalin, R. Wicaksono, and P. Arsil, "Aplikasi cabinet dryer (pengering kabinet) untuk meningkatkan produksi bahan baku pengawet alami buah kecombrang (etlingera elatior)," *Dinamika Journal: Pengabdian Masyarakat*, vol. 1, no. 3, 2019.

[4] P. B. Silva, G. D. Nogueira, C. R. Duarte, and M. A. Barrozo, "A new rotary dryer assisted by infrared radiation for drying of acerola residues," *Waste and Biomass Valorization*, vol. 12, pp. 3395–3406, 2021.

[5] S. Tarhan, S. Yıldırım, M. T. Tuncay, and İ. Telci, "Development of a rotary drum dryer to dry medicinal and aromatic plants," *Tarım Makinaları Bilimi Dergisi*, vol. 4, no. 3, pp. 295–300, 2008.

[6] W. Kaensup, S. Chutima, and S. Wongwises, "Experimental study on drying of chilli in a combined microwave-vacuum-rotary drum dryer," *Drying Technology - DRY TECHNOL*, vol. 20, pp. 2067–2079, 01 2002.

[7] T. Li, C. Li, B. Li, C. Li, Z. Fang, Z. Zeng, W. Ou, and J. Huang, "Characteristic analysis of heat loss in multistage counter-flow paddy drying process," *Energy Reports*, vol. 6, pp. 2153–2166, 11 2020.

[8] J. Ekka, K. Bala, P. Muthukumar, and D. Kanujiya, "Performance analysis of a forced convection mixed mode horizontal solar cabinet dryer for drying of black ginger (kaempferia parviflora) using two successive air mass flow rates," *Renewable Energy*, vol. 152, 06 2020.

[9] A. V. Pak, N. Pogozhikh, and A. O. Pak, "Development of an apparatus with induced heat-and-mass transfer for drying and hydrothermal processing of moist materials," *Eastern-European Journal of Enterprise Technologies*, vol. 3, no. 8, 2020.

[10] M. Abbes and A. Mami, "Modelling of a tunnel dryer with a bond graph approach," pp. 219–224, 07 2020.

[11] H. Oueslati, S. Mabrouk, and A. Mami, *Dynamic Modelling by Bond Graph Approach of Convective Drying Phenomena*. 02 2020.

[12] M. Ferney, "Modelling and controlling product manufacturing systems using bond-graphs and state equations: Continuous systems and discrete systems which can be represented by continuous models," *Production Planning & Control*, vol. 11, no. 1, pp. 7–19, 2000.

[13] J. K. Sagawa, M. S. Nagano, and M. S. Neto, "A closed-loop model of a multi-station and multi-product manufacturing system using bond graphs and hybrid controllers," *European Journal of Operational Research*, vol. 258, no. 2, pp. 677–691, 2017.

[14] A. Agrawal and P. Ghoshdastidar, "Computer simulation of heat transfer in a rotary lime kiln," *Journal of Thermal Science and Engineering Applications*, vol. 10, 02 2018.

[15] M. Eeom, T. Hahn, H. Lee, and S. Choi, "Performance analysis modeling for design of rotary kiln reactors," *Journal of the Korean Society of Combustion*, vol. 18, 09 2013.

[16] M. Piton, F. Huchet, O. Le Corre, L. Le Guen, and B. Cazacliu, "A coupled thermal-granular model in

flights rotary kiln: Industrial validation and process design," *Applied Thermal Engineering*, vol. 75, pp. 1011–1021, 2015.

[17] J. F. Broenink, "20-sim software for hierarchical bond-graph/block-diagram models," *Simulation Practice and Theory*, vol. 7, no. 5-6, pp. 481–492, 1999.